Available online at www.sciencedirect.com
SCIENCE DIRECT®
Applied Radiation and Isotopes 61 (2004) 179–183
Applied Radiation and Isotopes
www.elsevier.com/locate/apradiso

Background components of Ge detectors in Ogoya underground laboratory

Y. Hamajima*, K. Komura

LLRL, Kanazawa University, Tatsunokuchi 9231224, Japan

Abstract

Ogoya underground laboratory, (OUL; 270 m water equivalent), has 5 well, 4 planar, and 1 coaxial-type ultra-low background Ge detectors with passive shield of old lead. An anticoincidence system with a plastic scintillator (PS) has been tested to reduce cosmic-ray-induced background. Energy spectra of PSs, coincidence counting rate, and angular distribution of cosmic rays were studied. Based on this study, we propose a new index of Ge surface area-normalized background counting rate ($d^{-1}\,cm^{-2}$) to compare shielding efficiency between different types of Ge detectors.

Keywords: Ultra-low background; Underground laboratory; Gamma-ray measurement; Plastic scintillator; Cosmic ray

1. Introduction

Super Kamiokande is the most famous underground detector in Japan. This huge neutrino detector is located at 2700 m w.e. (meter water equivalent) depth of Kamioka mine in order to eliminate background component derived from cosmic ray. In gamma-ray measurements, it is also significant to reduce background derived from cosmic-ray components, activation of construction materials, and secondary neutrons. In early 1990s, the low background gamma-ray spectrometry by Ge detector was started at underground facility by many workers to detect double beta decay and dark matter as reviewed by Heusser (1995).

Ogoya is located about 70 km west from Kamioka, and 20 km southwest of Low Level Radioactivity Laboratory (LLRL), of Kanazawa University. There is a 546 m tunnel of former Ogoya copper mine, which was closed 40 years ago. We started the construction of the underground laboratory, OUL, in the tunnel at a distance of 290 m from the front entrance, where the overburden is 270 m w.e. (Komura, 1997). Some significant measurements have been performed at OUL such as detection of natural radionuclides induced by environmental neutrons (Komura and Yousef, 2000), assessment of neutron fluence by the JCO criticality accident at Tokai-mura in 1999 (Komura, 2001), and measurements of ultra-low level ^{152}Eu induced by Hiroshima Atomic Bomb (Komura et al., 2003).

OUL has 5 well (X, Y, C, W, and Z), 4 planar (J, K, I, and L), and 1 coaxial (U) Ge detectors, which are shielded with old lead. In this paper, background levels of ten Ge detectors are reported. We also propose a new background level index for normalization using the area of the detector crystal instead of the crystal mass, which is often reported. Finally, the performance of an active shield using plastic scintillators (PSs) with two different thicknesses is shown.

2. Background performances of Ge detectors with passive shield in OUL

In ultra-low background gamma-ray measurements, the radioactivity of the construction materials of the detector itself must carefully be selected (Heusser, 1995). For a typical detector in Ogoya ultra-low background aluminum was used for the end-cap. The cryostat is

*Corresponding author. Tel.: +81-761-51-4440; fax: +81-761-51-5528.

E-mail address: hama@cacheibm.s.kanazawa-u.ac.jp (Y. Hamajima).

0969-8043/$ - see front matter
doi:10.1016/j.apradiso.2004.03.041

J-shaped and the preamplifier is located outside the lead shield. The thickness of a lead shield is 20–25 cm, and the upper part of a shield is covered by 10–15 cm of iron. The inner 3–5 cm of a lead shield is composed of 200 years old lead. The space-near the detector head is filled with a Hg shield encapsulated in a polyethylene bag and nitrogen gas from the dewar is blown to the top of the end-cap.

After several days of measurement no peak, in addition to X-rays and 511 keV peak, was seen in any background spectrum from any of the 10 Ge detectors. Since the broad peaks of Ge(n, n′γ) and Pb(n, n′γ) excitation reactions in the 600–800 keV region were not found in the background spectrum, the influence of neutrons on the background spectrum is considered to be negligibly small.

In Table 1 the specifications and performances of Ge crystals and crystal area normalized background counting rate of the different detectors in OUL are shown.

2.1. Background index

The European network CELLAR reported background counting rates in different underground laboratories at different depths using a mass-normalized background index in $d^{-1}\,kg^{-1}$ (Hult et al., 2003). The background counting rate index of 800 $d^{-1}\,kg^{-1}$ of the coaxial detector-U in OUL fits well with their results considering that OUL is located 270 m w.e. under ground. On the other hand, the background counting rate of other types of detectors cannot be estimated simply by this index in spite of almost same shield condition.

As shown in Table 1, the planar detectors in OUL have large diameters and thicknesses of 2–3 cm in order to measure in a wide energy range from 20 keV to about 3 MeV. In close geometry measurements, they have usually higher absolute efficiencies at energies below 1 MeV compared to coaxial detectors of similar relative efficiency at 1.33 MeV. Therefore, background counting rates of planar-type Ge is inevitably higher than a coaxial-type with the same volume. On the other hand, even if well- and coaxial-type Ge-detectors have the same outer dimensions, the former has a smaller active volume but larger active area. For this reason, background counting rates of planar and well-type Ge-detectors cannot be well normalized simply by crystal mass.

It is expected for good background index that the same shielding conditions lead to the same grade of result, although the detector type is different. The background index normalized by surface area of Ge crystal [$d^{-1}\,cm^{-2}$] seems to be much better than the weight-normalized index [$d^{-1}\,kg^{-1}$]. At very deep laboratories where the background counting rate is dominated by radioactivity inside the Ge-crystal itself, it is, however, still of interest to use the crystal mass as normalization factor. The surface area was defined as the sum of the upper, the bottom, and the side area of cylindrical crystal. In the case of a well-type detector, the surface area of the well was neglected. The background index in $d^{-1}\,cm^{-2}$, thus normalized was shown in Table 1. It was found that this background index of planar (I, J, and K), well (C and W) and coaxial-type (U) Ge detectors were within the narrow range between 5.4 and 7.6. It should be noted that the indexes of J, K, W, and U

Table 1
Performance of Ge detectors in OUL

Ge	type[a]	Relative efficiency (%)	Diameter × Length (cm)	Useful volume[b] (cm^3)	BG[c] (min^{-1})	BG[d] ($d^{-1}\,kg^{-1}$)	BG[e] ($d^{-1}\,cm^{-2}$)[f]
I	Planar	18.2	5.9 ϕ × 2.0	56	0.48±0.01	2286±33	7.54±0.11
J	Planar	34	7.0 ϕ × 3.0	113	0.57±0.01	1345±18	5.74±0.08
K	Planar	34	7.0 ϕ × 3.0	113	0.52±0.01	1231±17	5.24±0.07
L	Planar	18.2	6.0 ϕ × 2.0	56	0.57±0.01	2714±36	8.78±0.12
X	Well (2.1 cm ϕ × 6 cm)	73	7.4 ϕ × 8.0	311	1.60±0.02	1359±11	8.43±0.07
Y	Well (2.1 cm ϕ × 6 cm)	70	7.4 ϕ × 8.0	314	1.75±0.02	1501±11	9.22±0.07
C	Well (1.0 cm ϕ × 4 cm)	37	6.1 ϕ × 5.6	151	0.82±0.01	1450±16	7.13±0.08
W	Well (2.1 cm ϕ × 6 cm)	65	7.5 ϕ × 8.0	344	1.20±0.02	930±8	6.21±0.06
Z	Well (1.6 cm ϕ × 6.2 cm)	52	6.8 ϕ × 7.0	231	(2.00±0.02)[g]	(2309±16)[g]	(13.07±0.09)[g]
U	Coaxial	93	7.9 ϕ × 8.1	379	1.12±0.02	788±7	5.41±0.05

[a] Diameter and length of well of end-cap shown in parenthesis.
[b] Same as sensitive volume.
[c] Integrated background count rate from 100 to 2000 keV.
[d] Integrated background count rate from 100 to 2000 keV normalized to the mass of detector crystal.
[e] Integrated background count rate from 100 to 2000 keV normalized to the surface area of detector crystal.
[f] Surface area (cm^2) of Ge is estimated as cylindrical shape of crystal.
[g] Preliminary result.

Table 2
Specifications of plastic scintillators

PS name	Size (mm^3)	Input	Output	Case
SCIONIX S	$400 \times 400 \times 50$	HV, preamp power	Energy	No
ALOKA A	$360 \times 310 \times 0.5$	+6 V	Slow positive NIM logic	1 mm/Al

were almost the same and rather higher background indexes were found for L, X, Y, and Z. These higher results were explained as contributions of residual activities, which might be produced by cosmic-ray interaction during high altitude flight from manufacturer to laboratory, and as these detectors were installed recently in OUL, such results have been observed. The index of about $5\,d^{-1}\,cm^{-2}$ is presumed to be a minimum (target) value in OUL.

3. Reduction of background components from cosmic ray by active shield

Since gamma-ray peaks derived from $(n, n'\gamma)$ reaction were not observed in the spectrum, muons are considered to be the major cosmic-ray component in OUL. As shown in Table 2, two types of PSs with almost the same size but with different thicknesses were examined in order to reduce the contribution of cosmic-ray components by anticoincidence system. The thick scintillator manufactured by SCIONIX (referred to as PS-S) was a conventional type PS with a photomultiplier tube (PMT). The thin scintillator from ALOKA (referred to as PS-A) was an experimental model with four PMTs, HV, and a SCA housed in the aluminum case, and the output was a slow positive NIM logic pulse. The upper and lower level thresholds of PS-A cannot be modified.

3.1. Energy spectrum of cosmic ray

In order to simplify the circuit, and to use the PS signal directly as an anticoincidence gate, it is desirable to discriminate the signal by cosmic ray from highly abundant gamma rays. Single (not coincidence) energy spectra of PS-S at 0 m w.e. (upper part) and at 270 m w.e. are shown in Fig. 1. Events below channel 100 were from Compton-scattered gamma rays and those above channel 200 were muon-induced pulses, which was reduced to about 1/100 at 270 m w.e. compared to above ground. We assumed that channel 150 corresponds to about 7 MeV and channel 600 to 25–30 MeV. The energy spectra of the muons in PS-S were quite broad and diffusing to both the low- and high-energy regions. Therefore, it is not easy to clearly cut out the gamma-ray components. Rise time discrimination of muons from gamma rays was also tried in a preliminary experiment, but a distinct difference of the rise times could not be observed.

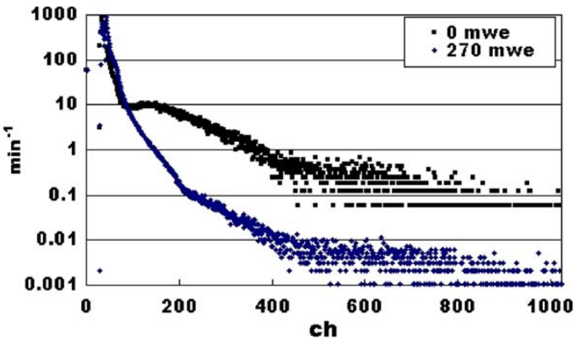

Fig. 1. The background counting rate (min^{-1}) as a function of energy (channel number) for PS-S at 0 m w.e. (upper, square) and at 270 m w.e. (lower, diamond) in OUL.

3.2. Thickness of PS

This experiment was performed at LLRL (ground level) to get large number of cosmic-ray event. Both PS-S and PS-A were set on the same top position of the thick shield of a coaxial-type Ge detector. Slow timing signals of PS-S or PS-A and Ge detector were led to a slow coincidence circuit. Coincidence events were recorded in multi-channel scaling mode. The counting rate of PS-A was almost equal to the estimated muon fluence ($1\,min^{-1}\,cm^{-2}$) at ground surface. It was found that most of the muons were detected with PS-A in spite of it being only a 0.5 mm thick scintillator. It was also found that most of the signals of PS-S were derived from environmental gamma rays.

Coincidence events between both PSs and the Ge-detector were compared. Coincidence counting rates were almost constant and independent on the thickness of PSs. The results suggest that 0.5 mm of PS is sufficient to detect cosmic-ray induced muons. It is favorable to use a thin PS as guard counter, because the counting rate arising from environmental gamma-rays is much lower compared with a thick PS. In addition a thin PS is easier to handle.

3.3. Angular distribution of cosmic ray

This experiment was performed at both OUL and LLRL. The angular distribution of coincidence events between a PS and a Ge-detector was measured as a function of zenith angle (θ). The setup was same as mentioned in Section 3.2.

Taking the finite cylindrical shape of the Ge-crystal into consideration, the solid angle of the PS and the coincidence counting rate in the unit of $min^{-1}\,sr^{-1}$ were calculated, and are shown in Fig. 2. The large uncertainties of the incident angle are due to the large width of PS that was used. The observed angler distribution of LLRL lies between the cos (θ) and the $\cos^2$ (θ) functions, which is consistent with the empirical function reported by Miyake (1973) shown by the dotted line. The observed value over 90° (backward) shows lower and close to the $\cos^3$ (θ) function.

It is known that the angular distribution of muons arriving at ground surface can be simulated using the $\cos^2$ (θ) function for higher energy components and the $\cos^3$ (θ) function for low energy ones. Present results show that PS pulses coincident with Ge-detector pulses are from the high energy muon component. The influence of the three-storeyed building (LLRL) and half-underground condition (about 1 m below ground level) of the Ge-detector used in the experiment must also be considered, because the observed angular distribution was not symmetric. The continuous background and the 511 keV peak observed in the coincidence spectrum (Fig. 3c) indicate that not only the muons but also cosmic-ray-induced and/or scattered high energy electrons, positrons, and bremsstrahlung radiation are detected as coincidence events.

The angular distribution in OUL (270 m w.e.) was quite different from that observed at LLRL. The maximum was observed at around 50°. This may be explained by the topography of overburden of the underground laboratory. The maximum at 50°

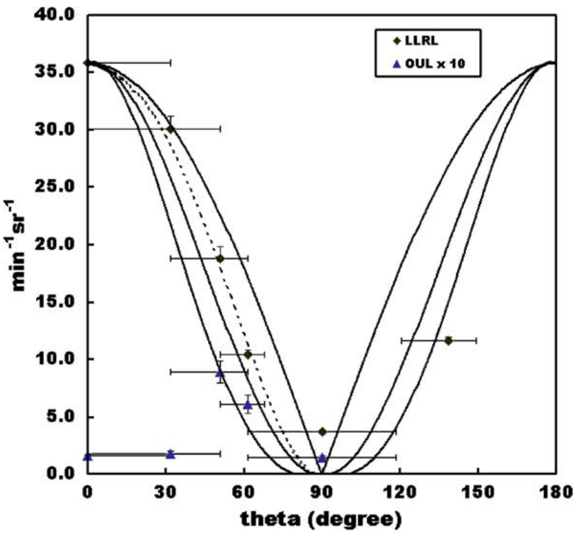

Fig. 2. Angular distribution of Ge and PS-A coincidence counting rate in OUL and LLRL. The solid angle of the PS was calculated taking into account the finite volume of the Ge-crystal. Note that the data of OUL is multiplied with a factor of ten. The absolute values of the cos (θ), $\cos^2$ (θ) and $\cos^3$ (θ) functions are shown as solid lines cos (θ) being the upper curve and $\cos^3$ (θ) being the bottom curve. The empirical function reported by Miyake (1973) is shown as a dotted line.

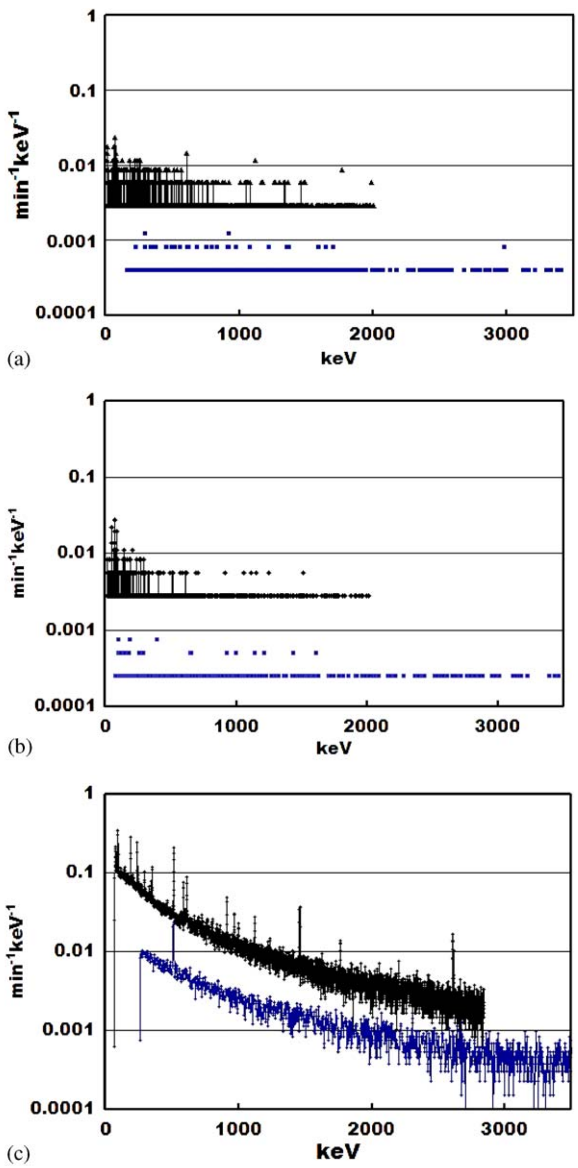

Fig. 3. Normal background (upper) and background with a PS in anticoincidence with the Ge-detector (lower) spectra of: (a) a typical coaxial Ge-detector at OUL, (b) a planar-type Ge at OUL and (c) a coaxial Ge-detector at LLRL.

corresponds to a nearby valley which reduces the shield for cosmic rays in that direction.

3.4. Coincidence gamma-ray spectrum with cosmic ray

The PS-A was set on the top of the shield of two kinds of detector in OUL, i.e. planer-type detector K and coaxial-type U, and a coaxial-type detector at LLRL. Coincidence and single spectra were measured, simultaneously, under the PS solid angle of 0.28 sr for U, 0.54 sr for K, and 0.23 sr for the detector at LLRL.

Single and coincident spectra measured in OUL are shown in Figs. 3(a) and (b) and that of LLRL in (c) for comparison. The PS-Ge coincidence spectra are shown in lower part and normal (singles) spectra in upper part. The integrated coincidence counting rate from 100 to 2000 keV is 0.084 min^{-1} for U and 0.040 min^{-1} for K. Surface area-normalized coincidence background counting rates are 0.40 and 0.41 $d^{-1} cm^{-2}$ for U and K, respectively. These values corresponded to 7.5% and 7.7% of the total background of the respective Ge-detectors. If a larger PS, which covers 2π geometry, is used for the anticoincidence shield, more than 30–40% of background reduction will be expected in OUL, though exact estimation for each detectors is undergoing.

An anticoincidence system with almost the same solid angle as the PS in OUL was applied to the ground level Ge-detector in LLRL. From this experiment, it was estimated that more than 90% of 511 keV gamma rays and continuous background components were removed by this system, assuming that angular distribution of muon was simulated by the $\cos^2(\theta)$ function.

4. Summary

1. A surface area-normalized background counting rate [$d^{-1} cm^{-2}$] is effective in comparing the background of different types of Ge detector. In OUL, about 5 $d^{-1} cm^{-2}$ was assumed to be the best value (target value).
2. The energy distribution of muons on the thick PS was broad and discrimination of muon events from gamma ray events was not easy for low-energy events.
3. The detection efficiency of muons did not depend on the thickness of PS so the thin PS with 0.5 mm thickness was sufficiently thick to detect muons.
4. The angler distribution of a muons in OUL has a maximum at around 50°. At ground level (LLRL), this distribution can be simulated with a function close to the $\cos(\theta)$ and $\cos^2(\theta)$ functions.
5. By using the anticoincidence system composed of one large area PS sitting on top of the Ge-detector 30–40% and 90% of background pulses can be reduced in OUL, and at LLRL, respectively.

Acknowledgements

Thanks are expressed to T. Yanai, Y. Ohta, and A. Iwamoto of ALOKA CO., LTD. for the preparation and tuning of thin plastic scintillator.

References

Heusser, G., 1995. Low radioactivity background techniques. Ann. Rev. Nucl. Part. Sci 45, 543–590.

Hult, M., Gasparro, J., Johnston, P.N., Köhler, M., 2003. Underground measurements of environmental radioactivity: European examples. Proc. Int. Symp. Kanazawa Univ. 21st Cent. COE Prog. 1, 18–23.

Komura, K., 1997. Challenge to detection limit of environmental radioactivity. Proceedings of the 1997 International Symposium on Environmental Radiation, Tsuruga, Fukui, Japan, October 20, pp. 56–75.

Komura, K., Yousef, A.M., 2000. Natural radionuclides induced by environmental neutrons. Proceedings of the International Workshop on Distribution and Speciation of Radionuclides in the Environment, Rokkasho, Aomori, Japan. October 11–13, pp. 210–217.

Komura, K., 2001. Radiochemical approach to the JCO criticality accident in Tokai-mura, 1999—an overview of the radiochemistry group. J. Radiat. Res. 42, S17–S29.

Komura, K., Hoshi, M., Endo, S., Imanaka, T., Fukushima, H., 2003. Ultra Low-background Measurement of ^{152}Eu in Hiroshima Samples. Private communication.

Miyake, S., 1973. Rapporteur paper on muons and neutrons. Proceedings of the 13th International Cosmic Ray Conference Report, Denver, Vol. 5, pp. 3638–3655.